

CONJUGATE FUNCTION METHOD AND CONFORMAL MAPPINGS IN MULTIPLY CONNECTED DOMAINS

HARRI HAKULA*, TRI QUACH†, AND ANTTI RASILA‡

Abstract. The conjugate function method is an algorithm for numerical computation of conformal mappings for simply and doubly connected domains. In this paper the conjugate function method is generalized for multiply connected domains. The key challenge addressed here is the construction of the conjugate domain and the associated conjugate problem. All variants of the method preserve the so-called reciprocal relation of the moduli. An implementation of the algorithm, along with several examples and illustrations are given.

Key words. numerical conformal mappings, conformal modulus, multiply connected domains, canonical domains

1. Introduction. Conformal mappings play an important role in both theoretical complex analysis and in certain engineering applications, such as electrostatics, aerodynamics, and fluid mechanics. Existence of conformal mappings of simply connected domains onto the upper-half plane or the unit disk follows from the Riemann mapping theorem, and there are generalizations of this result for doubly and multiply connected domains [2]. However, constructing such mappings analytically is usually very difficult, and numerical methods are required.

There exists an extensive literature on numerical construction of conformal mappings for simply and doubly connected domains [26]. One popular method is based on the Schwarz-Christoffel formula [12], and its implementation SC Toolbox is due to Driscoll [10, 11]. SC Toolbox itself is based on earlier FORTRAN package by Trefethen [29]. A new algorithm involving a finite element method and the harmonic conjugate function was presented by the authors in [14].

While the study of numerical conformal mappings in multiply connected domains dates back to 1980's [24, 27], recently there has been significant interest towards the subject. DeLillo, Elcrat and Pfaltzgraff [8] were the first to give a Schwarz-Christoffel formula for unbounded multiply connected domains. Their method relies on the Schwarzian reflection principle. Crowdy [4] was the first to derive a Schwarz-Christoffel formula for bounded multiply connected domains, which was based on the use of Schottky-Klein prime function. In a very recent paper [28] conformal maps from multiply connected domains onto lemniscatic domains have been discussed. The natural extension of this result to unbounded multiply connected domains is given in [5]. It should be noted that a MATLAB implementation of the Schottky-Klein prime function is freely available [6], and the algorithm is described in [7]. A method involving the harmonic conjugate function is given in [23], but the approach there differs from ours.

The foundation of conjugate function methods for simply and doubly connected domains lies on properties of the (conformal) modulus, which originates from the theory of quasiconformal mappings [1, 21, 26]. Here we extend the methods to multiply connected domains. In terms of partial differential equations, one has to solve the

*Aalto University, Institute of Mathematics, P.O. Box 11100, FI-00076 Aalto, FINLAND (harri.hakula@aalto.fi)

†Aalto University, Institute of Mathematics, P.O. Box 11100, FI-00076 Aalto, FINLAND (tri.quach@aalto.fi)

‡Aalto University, Institute of Mathematics, P.O. Box 11100, FI-00076 Aalto, FINLAND (antti.rasila@iki.fi)

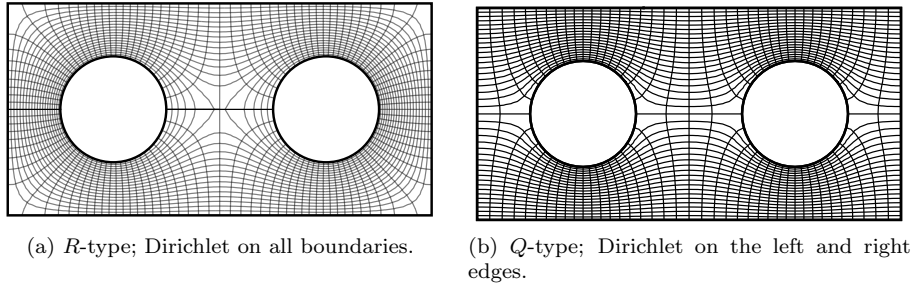


Fig. 1.1: Two Circles in Rectangle: Map.

Laplace equation $\Delta u = 0$, in Ω , with boundary conditions

$$\mathbf{1}_N \frac{\partial u}{\partial n} + \mathbf{1}_D u = f(x, y), \text{ on } \partial\Omega, \quad (1.1)$$

where the indicator functions refer to Neumann and Dirichlet boundary parts, respectively. Two configurations are of special interest: first, if only Dirichlet boundary conditions are set, e.g., 0 on the outer boundary, and 1 on the interior boundary components, the problem is ring-like, and second, if only two non-adjacent boundary segments have Dirichlet boundary conditions, the problem is quadrilateral-like; the configurations are referred to as types of *R* and *Q*, respectively (See Figure 1.1). In both cases the canonical domains are slit domains, first catalogued by Koebe [20].

The main result of this paper is the generalization of the of the algorithm for simply and doubly connected domains described in [14] to multiply connected ones with different boundary conditions. To our knowledge this is the first method for problems of type *R*. More specifically, the fundamental new result is the definition of the conjugate problem for multiply connected domains. We show formally for type *R* (Proposition 3.3) that this choice for the conjugate problem preserves the important reciprocal relation [21] for the moduli $M(\Omega)$ and $M(\tilde{\Omega})$ of the original and the conjugate problem, respectively:

$$M(\Omega)M(\tilde{\Omega}) = 1.$$

Similar result holds for type *Q*.

Our method is suitable for a very general class of domains, allowing curved boundaries and even cusps. The implementation of the algorithm is based on the *hp*-FEM described in [15], and in [16] it is generalized to cover unbounded domains. In [17], the method has been used to compute moduli of domains with strong singularities.

The performance of the method has been evaluated by solving four benchmark problems, two on computing resistances [9, 30], and two on capacities [3]. In each case the results agree with those obtained either with special-purpose methods or adaptive *h*-FEM.

In general, conformal mapping of multiply connected domains is possible only if the the domain is a conformal image of a Denjoy-domain, i.e., a domain complement of which is a subset of the real line. It is well-known that this property holds for any n times connected domain if n is 1, 2, or 3. In the method presented here, for instance in cases of type *R* the saddle points of the potential function of the original multiply

connected problem are special, and it may be that the mapping is not conformal exactly at the saddle point if the domain is not a Denjoy-domain. Thus, our method is conformal up to a finite set of points (*exceptional points*).

The rest of the paper is organized as follows: In Section 2 the necessary concepts from function theory are introduced. The new algorithms for multiply connected domains is described in Sections 3 and 4, for types of R and Q , respectively. After the numerical implementation is briefly discussed, an extensive set of numerical experiments is analyzed. As the final example of the paper we show how canonical domains can be used for tracking evolving solutions, e.g., stress fields, as the computational domain is perturbed.

2. Preliminaries. In this section we introduce concepts from function theory and review the algorithm for simply or doubly connected domains. For details and references we refer to [14].

DEFINITION 2.1. (*Modulus of a Quadrilateral*)

A Jordan domain Ω in \mathbb{C} with marked (positively ordered) points $z_1, z_2, z_3, z_4 \in \partial\Omega$ is called a quadrilateral, and denoted by $Q = (\Omega; z_1, z_2, z_3, z_4)$. Then there is a canonical conformal map of the quadrilateral Q onto a rectangle $R_d = (\Omega'; 1 + id, id, 0, 1)$, with the vertices corresponding, where the quantity d defines the modulus of a quadrilateral Q . We write

$$M(Q) = d.$$

Notice that the modulus d is unique.

LEMMA 2.2. (*Reciprocal Identity*)

The following reciprocal identity holds:

$$M(Q) M(\tilde{Q}) = 1, \tag{2.1}$$

where $\tilde{Q} = (\Omega; z_2, z_3, z_4, z_1)$ is called the conjugate quadrilateral of Q .

2.1. Dirichlet-Neumann Problem. It is well known that one can express the modulus of a quadrilateral Q in terms of the solution of the Dirichlet-Neumann mixed boundary value problem.

Let Ω be a domain in the complex plane whose boundary $\partial\Omega$ consists of a finite number of piecewise regular Jordan curves, so that at every point, except possibly at finitely many points of the boundary, an exterior normal is defined. Let $\partial\Omega = A \cup B$ where A, B both are unions of regular Jordan arcs such that $A \cap B$ is finite. Let ψ_A, ψ_B be real-valued continuous functions defined on A, B , respectively. Find a function u satisfying the following conditions:

1. u is continuous and differentiable in $\overline{\Omega}$.
2. $u(t) = \psi_A(t)$, for all $t \in A$.
3. If $\partial/\partial n$ denotes differentiation in the direction of the exterior normal, then

$$\frac{\partial}{\partial n} u(t) = \psi_B(t), \quad \text{for all } t \in B.$$

The problem associated with the conjugate quadrilateral \tilde{Q} is called the *conjugate Dirichlet-Neumann problem*.

Let $\gamma_j, j = 1, 2, 3, 4$ be the arcs of $\partial\Omega$ between $(z_1, z_2), (z_2, z_3), (z_3, z_4), (z_4, z_1)$, respectively. Suppose that u is the (unique) harmonic solution of the Dirichlet-Neumann problem with mixed boundary values of u equal to 0 on γ_2 , equal to 1

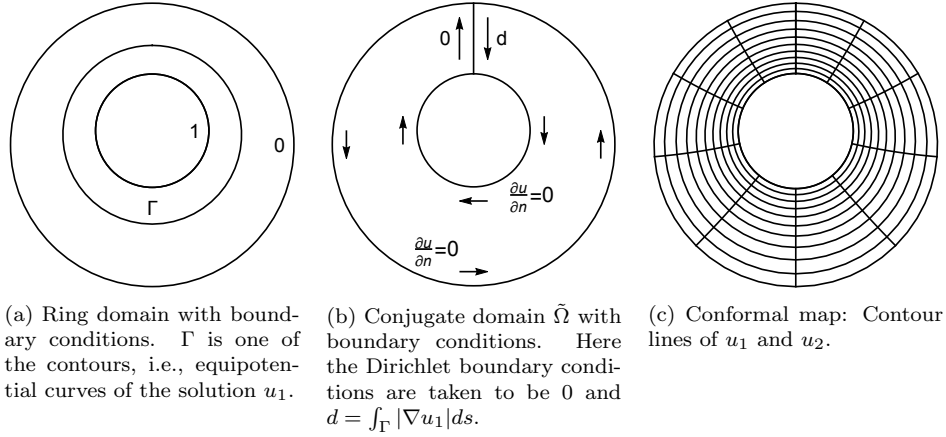


Fig. 2.1: Introduction to the conjugate function method for ring domains.

on γ_4 , and $\partial u / \partial n = 0$ on γ_1, γ_3 . Then:

$$M(Q) = \iint_{\Omega} |\nabla u|^2 dx dy. \quad (2.2)$$

Suppose that Q is a quadrilateral, and u is the harmonic solution of the Dirichlet-Neumann problem and let v be a conjugate harmonic function of u , $v(\operatorname{Re} z_3, \operatorname{Im} z_3) = 0$. Then $f = u + iv$ is an analytic function, and it maps Ω onto a rectangle R_h such that the image of the points z_1, z_2, z_3, z_4 are $1 + id, id, 0, 1$, respectively. Furthermore by Carathéodory's theorem, f has a continuous boundary extension which maps the boundary curves $\gamma_1, \gamma_2, \gamma_3, \gamma_4$ onto the line segments $\gamma'_1, \gamma'_2, \gamma'_3, \gamma'_4$.

LEMMA 2.3. *Let Q be a quadrilateral with modulus d , and let u be the harmonic solution of the Dirichlet-Neumann problem. Suppose that v is the harmonic conjugate function of u , with $v(\operatorname{Re} z_3, \operatorname{Im} z_3) = 0$. If \tilde{u} is the harmonic solution of the Dirichlet-Neumann problem associated with the conjugate quadrilateral \tilde{Q} , then $v = d\tilde{u}$.*

2.2. Ring Domains. Let E_0 and E_1 be two disjoint and connected compact sets in the extended complex plane $\mathbb{C}_{\infty} = \mathbb{C} \cup \{\infty\}$. Then one of the set E_0 or E_1 is bounded and without loss of generality we may assume that it is E_0 . Then a set $R = \mathbb{C}_{\infty} \setminus (E_0 \cup E_1)$ is connected and is called a *ring domain*. The *capacity* of R is defined by

$$\operatorname{cap} R = \inf_u \iint_R |\nabla u|^2 dx dy,$$

where the infimum is taken over all non-negative, piecewise differentiable functions u with compact support in $R \cup E_0$ such that $u = 1$ on E_0 . Suppose that a function u is defined on R with 1 on E_0 and 0 on E_1 . Then if u is harmonic, it is unique and it minimizes the integral above. The conformal modulus of a ring domain R is defined by $M(R) = 2\pi / \operatorname{cap} R$. The ring domain R can be mapped conformally onto the annulus A_r , where $r = M(R)$.

2.3. Conjugate Function Method. For simply connected domains the conjugate function method can be defined in three steps.

ALGORITHM 2.4. (*Conjugate Function Method*)

1. Solve the Dirichlet-Neumann problem to obtain u_1 and compute the modulus d .
2. Solve the Dirichlet-Neumann problem associated with \tilde{Q} to obtain u_2 .
3. Then $f = u_1 + idu_2$ is the conformal mapping from Q onto R_d such that the vertices (z_1, z_2, z_3, z_4) are mapped onto the corners $(1 + id, id, 0, 1)$.

For ring domains the algorithm has to be modified, of course, and here the fundamental step is the cutting of the domain along the path of steepest descent, which enables us to return the problem to similar settings as for the simply connected case.

ALGORITHM 2.5. (*Conjugate Function Method for Ring Domains*)

1. Solve the Dirichlet problem to obtain the potential function u and the modulus $M(R)$.
2. Cut the ring domain through the steepest descent curve which is given by the gradient of the potential function u_1 and obtain a quadrilateral where the Neumann condition is on the steepest descent curve and the Dirichlet boundaries remain as before.
3. Use the method for simply connected domains (Algorithm 2.4).

Notice that the choice of the steepest descent curve is not unique due to the implicit orthogonality condition. In Figure 2.1 an example of the ring domain case is given. The key observation is that $d = \int_{\Gamma} |\nabla u_1| ds$, where Γ is any of the contour lines of the solution u_2 . In Figure 2.1b the Dirichlet boundary conditions are set to be 0 and d , instead of usual choice of 0 and 1. This choice does not have any effect for Figure 2.1c but is of paramount interest in the generalization of the algorithm.

DEFINITION 2.6 (Cut). *A cut γ is a curve in the domain Ω , which introduces two boundary segments denoted by γ^+ and γ^- to the conjugate domain $\tilde{\Omega}$. Along the oriented boundary $\partial\tilde{\Omega}$, the segments γ^+ and γ^- are traversed in opposite directions.*

For the sake of discussion below let us define the conjugate problem directly. The cut γ (Definition 2.6) has its end points on ∂E_0 and ∂E_1 . One choice for the (oriented) boundary of conjugate domain $\tilde{\Omega}$ starting from the end point of γ on ∂E_1 is given by the set $\{\gamma^+, \partial E_0, \gamma^-, \partial E_1\}$ as shown in Figure 2.1b. The boundary conditions are set as $u = 0$ on γ^+ , $u = d$ on γ^- , and $\partial u_2 / \partial n = 0$ on ∂E_j , $j = 1, 2$.

2.4. Canonical Domains. The so called canonical domains play a crucial role in the theory of quasiconformal mappings (cf. [21]). These domains have a simple geometric structure. Let us consider a conformal mapping $f: \Omega \rightarrow D$, where D is a canonical domain, and Ω is the domain of interest. The choice of the canonical domain depends on the connectivity of the domain Ω , and both domains D and Ω have the same connectivity. It should be noted that in simply and doubly connected cases, domains can be mapped conformally onto each other if and only if their moduli agree. In this sense, moduli divide domains into conformal equivalence classes. For simply connected domains, natural choices for canonical domains are the unit disk, the upper half-plane and a rectangle. In the case of doubly connected domains an annulus is used as the canonical domain. For m -connected domains, $m > 2$, we have $3m - 6$ different moduli, which leads to various choices of canonical domains. These domains have been studied in [13, 25]. The generalization of Riemann mapping theorem onto multiply connected domains is based on these moduli, see [13, Theorems 3.9.12, 3.9.14].

3. Conjugate Function Method for Multiply Connected Domains of Type R . Let us first formally define the multiply connected domains of type R and their capacities. Let $m > 2$ and E_0, E_1, \dots, E_m be disjoint and nondegenerate

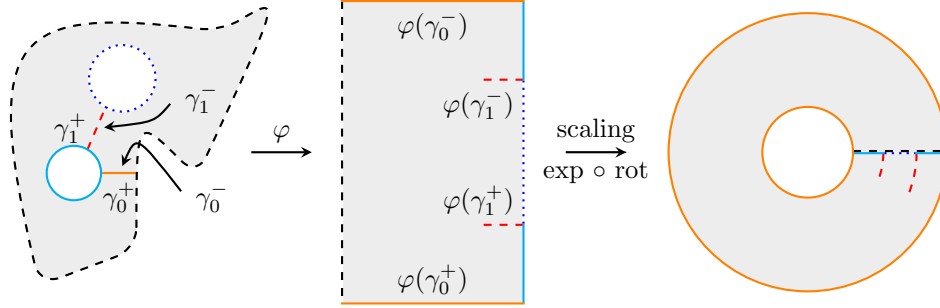


Fig. 3.1: Construction of the conformal mapping from the domain of interest onto a canonical domain. In the first part, we use Algorithm 3.5, which creates the orange cut γ_0 and the dashed red cut γ_1 . In the algorithm these cuts are traversed twice, which lead to two separated line-segments $\varphi(\gamma_k^+)$ and $\varphi(\gamma_k^-)$ on the rectangle. The latter part consist of a rotation, a scaling, and finally mapping with the exponential function.

continua in the extended complex plane $\mathbb{C}_\infty = \mathbb{C} \cup \{\infty\}$. Suppose that E_j , $j = 1, 2, \dots, m$ are bounded, then a set $\Omega_{m+1} = \mathbb{C}_\infty \setminus \bigcup_{j=0}^m E_j$ is $(m+1)$ -connected domain, and its (conformal) capacity is defined by

$$\text{cap } \Omega_{m+1} = \inf_u \iint_{\Omega_{m+1}} |\nabla u|^2 dx dy,$$

where the infimum is taken over all non-negative, piecewise differentiable functions u with compact support in $\bigcup_{j=1}^m E_j \cup \Omega_{m+1}$ such that $u = 1$ on E_j , $j = 1, 2, \dots, m$. Suppose that a function u is defined on Ω_{m+1} with 1 on E_j , $j = 1, 2, \dots, m$ and 0 on E_0 . Then if u is harmonic, it is unique, and it minimizes the integral above. The modulus of Ω_{m+1} is defined by $M(\Omega_{m+1}) = 2\pi/\text{cap } \Omega_{m+1}$. If the degree of connectivity does not play an important role, the subscript will be omitted and we simply write Ω .

In contrast with the ring problem there is no immediate way to define a conjugate problem. Indeed, it is clear that the conjugate domain *cannot* be a quadrilateral in the sense of definitions above. However, there exists a contour line Γ_0 such that it encloses the set E_j , $j = 1, 2, \dots$, and

$$d = M(\Omega_{m+1}) = \int_{\Gamma_0} |\nabla u| ds. \quad (3.1)$$

Thus, there is an analogue for the cutting of the domain along the curve of steepest descent. It can be assumed without any loss generality, that the cut γ_0 (and the Dirichlet conditions) is between E_0 and E_1 . Then the immediate question is how to cut the domain further between E_j , $j = 1, 2, \dots, m$, in such a fashion that the conjugate domain is simply connected, and set the boundary conditions so that the Cauchy-Riemann equations are satisfied?

There is one additional property of the solution u that we can utilize. Namely, for every E_j , $j = 1, 2, \dots$, there exists an enclosing contour line Γ_j . The capacity has

a natural decomposition

$$d = \sum_j \hat{d}_j, \quad \hat{d}_j = \int_{\Gamma_j} |\nabla u| ds = \sum_k d_k = \sum_k \int_{\Gamma_{j,k}} |\nabla u| ds, \quad (3.2)$$

where $\Gamma_{j,k}$ denotes a segment from discretization of the contour line $\Gamma_j = \cup_k \Gamma_{j,k}$.

3.1. Saddle Points. The saddle points of the solution u are of special interest. Notice that for simply and doubly connected domains they do not exist, thus any generalization of the Algorithm 2.4 must address them specifically. First, there are two steepest-descent curves emanating from every saddle point. This means that in the conformal mapping of the domain slits will emerge since the potential at the saddle point must be less than 1. Second, analogously there are two steepest/ascent curves reaching some boundary points z_i, z_j , at boundaries $\partial E_i, \partial E_j$, respectively. In addition, we say that E_i and E_j are conformally visible to each other.

REMARK 1. *For symmetric configurations there may be more than two steepest-descent and steepest-ascent curves at the saddle point.*

3.2. Cutting Process. The orthogonality requirement implies that the curve formed by joining two curves of steepest descent from E_i and E_j meeting at the saddle point must be a contour line of the conjugate solution, that is, an equipotential curve. It follows that as in the doubly connected case, both boundary segments induced by a cut have a different Dirichlet condition. Therefore the cutting process can be outlined as follows:

ALGORITHM 3.1. (*Cutting Process*)

1. *Identify the saddle points $s_k, k = 1, 2, \dots$*
2. *Join the two curves of steepest descent from ∂E_i and ∂E_j meeting at the point s_k into cut $\gamma_m, m \geq 1$.*
3. *Starting from the first cut, form an oriented boundary of a simply connected domain by alternately traversing cuts γ_m and segments of ∂E_j induced by the cuts. Once the boundary is completed, every cut has been traversed twice (in opposite directions) and every ∂E_j has been traversed once.*

In Figure 3.2 two configurations are shown.

REMARK 2. *The symmetric case is covered if we allow for overlapping or partially overlapping cuts.*

3.3. Dirichlet Conditions Over Cuts. Once the domain Ω has been cut and the oriented boundary of the conjugate domain $\tilde{\Omega}$ has been set up it remains to set the Dirichlet conditions over the cuts. Given that the first cut leads to boundary conditions of 0 and d , it is sufficient to simply trace the oriented boundary of $\tilde{\Omega}$ and maintain the cumulative sum of jumps in modules computed over the segments $\Gamma_{j,k}$ connecting two consecutive cuts. Referring to Figure 3.2 notice that the identity (3.2) hold over the segments $\Gamma_{j,k}$.

ALGORITHM 3.2. (*Dirichlet Conditions Over Cuts*)

1. *Set the Dirichlet boundary conditions of the boundary conditions induced by the first cut to 0 and d .*
2. *Trace the boundary starting from the zero boundary and update the cumulative sum of*

$$d_m = \int_{\Gamma_{j,k}} |\nabla u| ds,$$

where the $\Gamma_{j,k}$ are included in the order given by the boundary orientation.

3. At every cut set the Dirichlet condition to the cumulative sum reached at that point.

3.4. Reciprocal Identity. Suppose that u_1 is the (unique) harmonic solution of the Dirichlet-Neumann problem given in the beginning of Section 3. Let u_2 be a conjugate harmonic function of u_1 such that $u_2(\operatorname{Re} \tilde{z}, \operatorname{Im} \tilde{z}) = 0$, where \tilde{z} is the intersection point of E_0 and γ_0^+ .

Then $\varphi = u_1 + iu_2$ is an analytic function, and it maps Ω onto a rectangle $R_d = \{z \in \mathbb{C} : 0 < \operatorname{Re} z < 1, 0 < \operatorname{Im} z < d\}$ minus $n - 2$ line-segments, parallel to real axis, between points $(u_1(\tilde{z}_j), d_j)$ and $(1, d_j)$, where \tilde{z}_j is the saddle point of the corresponding j th jump. In the process we have total of n jumps. See Figure 3.1 for an illustration of a triply connected example.

Let u_2 be the harmonic solution satisfying following boundary values u_2 equal to 0 on γ_0^+ and equal to 1 on γ_0^- , Neumann conditions $\partial u_2 / \partial n = 0$ on ∂E_j , $j = 0, 1, \dots, m$. For the cutting curves γ_j , $j = 1, 2, \dots, m$, we have Dirichlet condition and the value is the cumulative sum $\sum_{j=0}^m d_j$. On the n th jump, we have on the corresponding cutting curve γ_j

$$u_2 = \frac{\sum_{j=0}^n d_j}{d},$$

where d_j are given by (3.2). Note that, if Γ_0 is an equipotential curve from γ_0^+ to γ_0^- , then we have

$$M(\tilde{\Omega}) = \int_{\Gamma_0} |\nabla u_2| ds = \frac{1}{d}.$$

Thus we have a following proposition, which has the same nature as the reciprocal identity given in [15].

PROPOSITION 3.3 (Reciprocal identity). *Suppose u_1 and u_2 are the solutions to problems on Ω and $\tilde{\Omega}$, respectively. If $M(\Omega)$ denotes the integral of the absolute value of gradient of u_2 over the equipotential curve from γ_0^+ to γ_0^- , and $M(\tilde{\Omega})$ denotes the same integral for u_2 , then we have a normalized reciprocal identity*

$$M(\Omega)M(\tilde{\Omega}) = 1, \tag{3.3}$$

This reciprocal identity can be used in measuring the relative error of conformal mapping. It should be noted, that the mapping depends on $3m - 6$ parameters, moduli. Thus, theoretically it is possible to have an incorrect result for some of the moduli such that the reciprocal identity holds. However, probability of consistently having incorrect moduli for significant applications is extremely low.

LEMMA 3.4. *Let Ω be a multiply connected domain and let u be the harmonic solution of the Dirichlet-Neumann problem. Suppose that v is the harmonic conjugate function of u such that $v(\operatorname{Re} \tilde{z}, \operatorname{Im} \tilde{z}) = 0$, where \tilde{z} is the intersection point of E_0 and γ_0^+ , and d is a real constant given by (3.1). If \tilde{u} is the harmonic solution of the Dirichlet-Neumann problem associated with the conjugate problem of Ω , then $v = d\tilde{u}$.*

Proof. It is clear that v, \tilde{u} are harmonic. By Cauchy-Riemann equations, we have $\langle \nabla u, \nabla v \rangle = 0$. We may assume that the gradient of u does not vanish on ∂E_j , $j = 0, 1, \dots, m$. Then on ∂E_0 , we have $n = -\nabla u / |\nabla u|$, where n denotes the exterior normal of the boundary. Likewise, we have $n = \nabla u / |\nabla u|$ on ∂E_j , $j = 1, 2, \dots, m$. Therefore

$$\frac{\partial v}{\partial n} = \langle \nabla v, n \rangle = \pm \frac{1}{|\nabla u|} \langle \nabla v, \nabla u \rangle = 0.$$

On the cutting curves, we have from Cauchy-Riemann equations $|\nabla u| = |\nabla v|$, and from the jumping between cutting curves that $d = \sum_{j=0}^n d_j$. These results together imply that on the n th jump, we have on the corresponding cutting curve γ_k

$$v = \sum_{j=0}^n d_j.$$

Then by the uniqueness theorem for harmonic functions [2, p. 166], we conclude that $v = d\tilde{u}$.

Lastly, the proof of univalence of $\varphi = u + iv$ follows from the proof of univalence of f in [14, Lemma 2.3]. \square

3.5. Outline of the Algorithm. For convenience we use $\{\gamma\}$ and $\{\partial E\}$ to denote the sets of all cuts and boundaries, respectively.

ALGORITHM 3.5. (*Conjugate Function Method for Multiply Connected Domains of type R*)

1. Solve the Dirichlet problem to obtain the potential function u_1 and the modulus $d = M(\Omega)$.
2. Choose one path of steepest descent reaching the outer boundary E_0 , γ_0 .
3. Identify the saddle points s_m .
4. For every saddle point: Find paths γ_k , $k > 1$, joining two conformally visible boundaries ∂E_i and ∂E_j by finding the paths of steepest descent meeting at the point s_m .
5. For every E_i : Choose a corresponding contour Γ_i , compute its subdivision $\Gamma_{i,k}$ induced by the paths $\{\gamma\}$, and the corresponding jumps $d_k = \int_{\Gamma_{i,k}} |\nabla u| ds$.
6. Construct the conjugate domain $\tilde{\Omega}$ by forming an oriented boundary using paths $\{\gamma\}$ and $\{\partial E\}$.
7. Set the boundary conditions along paths $\{\gamma\}$ by accumulating jumps in the order of traversal.
8. Solve the Dirichlet-Neumann problem on $\tilde{\Omega}$ for u_2 .
9. Construct the conformal mapping $\varphi = u_1 + idu_2$.

3.6. Moduli and Degree of Freedom. For $m+1$ connected domains, we have $3m-3$ different moduli, degrees of freedom. In general, we have $2m-1$ jumps, and $m-1$ saddle points. This sums up to $3m-2$. However the cut γ_0 can be chosen so that the first and the last jumps, d_1 and d_{2m-1} , respectively, are equal. Thus the number of degrees of freedom is reduced by one, and we obtain $3m-3$.

4. Conjugate Function Method for Multiply Connected Domains of Type Q. Let us next focus on the quadrilateral-like case, i.e., type Q . Conceptually the construction is much simpler than that of type R . Let the exterior boundary ∂E_0 be composed of four arcs in the sense of Section 2.1 above, and the interior boundaries ∂E_j , $j = 1, \dots, m$, have Neumann boundary conditions $\partial u / \partial n = 0$. Intuitively it is clear that the definition of the conjugate problem has to involve a Dirichlet-Neumann map, and that there is no need for any cutting process. Once the potentials over ∂E_j , $j = 1, \dots, m$, have been defined for the conjugate problem, the reciprocal identity follows immediately.

4.1. Dirichlet Conditions Over Interior Boundaries. Let us consider the configuration of Figure 4.1. In the initial problem the Dirichlet boundary conditions are $u = 1$ and $u = 0$ on left and right hand edges, respectively. On every interior

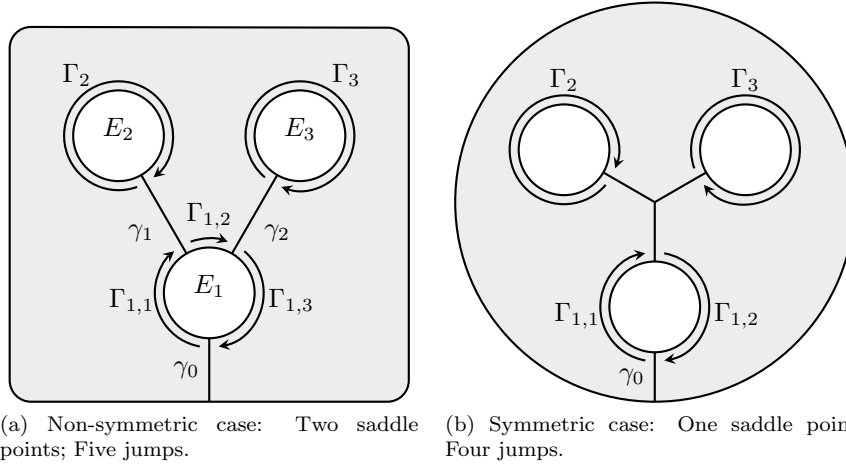


Fig. 3.2: Examples of non-symmetric and symmetric domains with cuts γ and decomposition of jumping curves $\Gamma_{i,k}$.

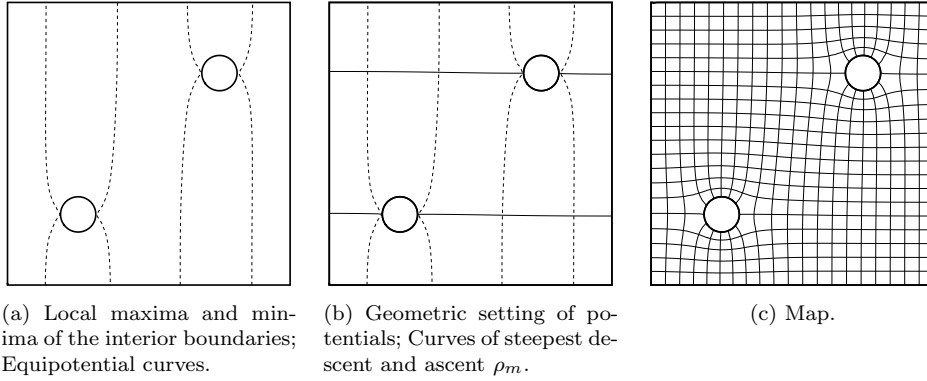


Fig. 4.1: Q -type: Dirichlet conditions for the conjugate problem: Initially on the left hand edge $u = 1$ and right hand edge $u = 0$.

boundary ∂E_j , $j = 1, \dots, m$, there are exactly two points with unique potentials that correspond to local maxima and minima, Figure 4.1a. Let us consider ∂E_j and denote the point with maximum potential x . Point x is connected with a point s on either one of the Dirichlet boundaries via a curve of steepest ascent ρ , Figure 4.1b. In the conjugate problem, the Dirichlet boundaries become Neumann ones. Along the Neumann edges the solution will be linear and have all values in the interval $[0, 1]$. Thus, the potential at the point s , and by construction at x since ρ is an equipotential curve in the conjugate problem, can be found using simple interpolation. The same procedure can be applied to the point of local minimum on ∂E_j . The resulting map is given in Figure 4.1c.

4.2. Outline of the Algorithm. Let us assume that in the initial Dirichlet-Neumann problem, along the boundary segment γ_1 the Dirichlet boundary condition is $u = 1$.

ALGORITHM 4.1. (*Conjugate Function Method for Multiply Connected Domains of type Q*)

1. Solve the Dirichlet-Neumann problem to obtain the potential function u_1 and the modulus $d = M(\Omega)$.
2. Locate the local maxima and minima on the interior boundaries ∂E_j , $j = 1, \dots, m$.
3. For every local maximum x_m : Find paths of steepest ascent ρ_m , $m > 1$, connecting x_m on ∂E_i with the point s_m on γ_1 .
4. Interpolate the potential on s_m on γ_1 when γ_1 is a Neumann edge.
5. Construct the conjugate domain $\tilde{\Omega}$ by performing the Dirichlet-Neumann map on ∂E_0 and setting the Dirichlet boundary conditions on ∂E_j , $j = 1, \dots, m$, to values obtained in the previous step.
6. Solve the Dirichlet-Neumann problem on $\tilde{\Omega}$ for u_2 .
7. Construct the conformal mapping $\varphi = u_1 + idu_2$.

5. Numerical Implementation of the Algorithms. We use the implementation of the *hp*-FEM method described in detail in [15]. The strategy for computing the equipotential lines from the canonical domain onto the domain of interest can be found in [14].

The main difference between the two algorithms are the cuts between the sets E_j , $j = 1, 2, \dots, m$ in the case of type *R*, especially locating the saddle point between sets. We use the Ridge method, proposed by Ionova and Carter [19], to locate the saddle points.

To find the actual cutting curve, we bisect ∂E_j , $j = 1, \dots, m$ and move against the gradient of u . By doing so, we search for a point on ∂E_j such that we end up within a tolerance from the saddle point.

If the cut can be computed analytically, the cut line can be embedded in the *a priori* mesh and thus the same mesh can be used in both problems. In this situation it is sufficient to perform elemental integration once. The common blocks in the assembled linear systems can be eliminated as in [14, Section 4.2]. In the general case, where the cutting has to be computed numerically the meshes may vary over large regions and the positive bias from reusing the mesh is lost. In the numerical experiments below we have used different refinements in two cases in order to test the sensitivity of the algorithm to mild perturbations of the mesh. The numerical algorithm is outlined in Figure 5.1.

For the *Q*-type, similar iteration can be used to refine the potential values. In this case it may be necessary to refine the geometric search for the potential values.

6. Numerical Experiments. In this section we discuss a series of benchmark problems and experiments carefully designed to illustrate different aspects of the algorithms. In electrostatics the *Q*-type refers to resistor design problems with multiple voltage domains and the *R*-type to capacitor (electrical condenser) design ones. In practice, designing integrated circuits multiple voltage domains is labor intensive and there is a need for advanced design systems [18]. We have selected two problems of both types from literature and designed the experiments for *R*-type since to our knowledge there are no reported benchmark problems with the actual maps for the *R*-type domains.

```

Data: Domain  $\Omega$ , tolerances  $\epsilon_i$ ,  $i = 1, \dots, 4$  for the  $M(\Omega)$ , saddle point, cuts,
        and the reciprocal error, respectively.
1 Discretize the domain  $\Omega$ , solve  $u_1$  and compute  $M(\Omega)$  with the desired
  tolerance  $\epsilon_1$ ;
2 while True do
3   | Locate the saddle points (within tolerance  $\epsilon_2$ );
4   | Search the cuts (within tolerance  $\epsilon_3$ );
5   | Discretize the domain  $\tilde{\Omega}$ , solve  $u_2$ , and compute  $M(\tilde{\Omega})$ ;
6   | if The reciprocal error is below tolerance  $\epsilon_4$  then break;
7   | Decrease tolerances for the saddle points and the cuts,  $\epsilon_2$  and  $\epsilon_3$ ,
    | respectively;
8 end

```

Fig. 5.1: *R*-type: High-level description of the numerical algorithm.

The use of the reciprocal relation as an error measure is formalized in the following definition:

DEFINITION 6.1 (Reciprocal error). *Using Proposition 3.3 we can define two versions of the reciprocal error. First for non-normalized jumps*

$$e_r^d = |1 - M(\Omega)/M(\tilde{\Omega})|, \quad (6.1)$$

and second for the normalized ones

$$e_r^n = |1 - M(\Omega)M(\tilde{\Omega})|. \quad (6.2)$$

and for convenience an associated error order

DEFINITION 6.2 (Error order). *Given a reciprocal error e_r^* , the positive integer e_i ,*

$$e_i = \lceil \log(e_r^*) \rceil, \quad (6.3)$$

is referred to as the error order.

Within the experiments we first consider cases with symmetries where the cut can be computed analytically, and then a general case with two saddle points (extraordinary points). We are interested in convergence in the energy norm as well as pointwise convergence.

For the general case the use of reciprocal error is not straightforward, however. The cuts must be approximated numerically and the related approximation error leads to inevitable *consistency error* since the jumps depend on the chosen cuts. Thus, in order to have a similar confidence in the general case as for the symmetric cases, one should consider a sequence of approximations for the cuts as outlined above (Figure 5.1). Here, however, we are content to show via the conformal map that the chosen cut is a reasonable one, and the resulting map has the desired characteristics.

Of course, the exact potential functions are not known. However, we can always compute contour plots of the quantities of interest, that is, the absolute values of the derivatives, and get a qualitative idea of the overall performance of the algorithm. Naturally, this also measures the pointwise convergence of the Cauchy-Riemann problem.

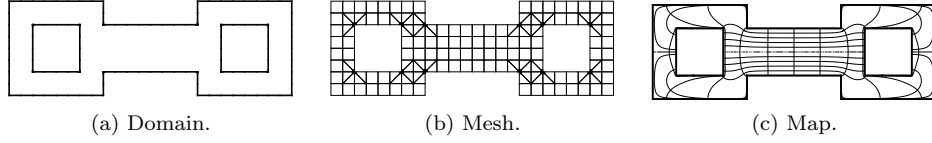


Fig. 6.1: Interior contacts.

Data on benchmarks and experiments, including representative numbers for degrees of freedom assuming constant $p = 12$, is given in Table 6.1 and Table 6.2c, respectively. In all cases the setup of the geometry is the most expensive part in terms of human effort and time. As is usual in hp -FEM, the computational cost in these relatively small systems is in integration and handling of the sparse systems. The actual computations take minutes on standard desktop hardware using our implementation of the algorithms.

6.1. Benchmarks. In [30] Trefethen gives an excellent introduction to the connection between conformal maps and computation of resistances of idealized planar resistors. In our setting the quantity of interest, the resistance of the resistor, is equal to the modulus of the conjugate domain.

6.1.1. Computation of resistances for interior contacts. Our first benchmark, Figure 6.1, is a symmetric triply connected bar. On the interior square boundaries we have Dirichlet boundary conditions and on the outer boundary Neumann ones. In the context of the application, the voltages are applied on the interior and the exterior is insulated. This example was first discussed in [30] where the computation were carried out with simply connected Schwarz-Christoffel transformations by exploiting the symmetry to subdivide the domain into four simply connected domains. In [9] the same problem is computed using the method of DeLillo et al. [8] without exploiting the symmetry.

The domain is enclosed by $B = [0, 3] \times [-1/2, 1/2]$. There are two square holes

$$H_1 = [1/4, 3/4] \times [-1/4, 1/4], \quad H_2 = [9/4, 11/4] \times [-1/4, 1/4],$$

and indentations

$$I_1 = [1, 2] \times [-1/2, -1/4], \quad I_2 = [1, 2] \times [1/4, 1/2].$$

The domain $\Omega = B \setminus (H_1 \cup H_2 \cup I_1 \cup I_2)$. This problem is neither of type R nor Q . Since the contacts are on the interior boundaries, cuts with Dirichlet conditions must be present in the conjugate problem. Here we cut along $y = 0$, set $u = 0$, if $1 \leq x \leq 2$ and $u = \pm 1/2$ otherwise.

The computed value of resistance $R = 2.768867502692$ is equal to those reported in [30] and [9]. Notice that in Figure 6.1c, the maps include details also around the contacts.

6.1.2. Computation of resistances for quadrilaterals. Our second benchmark is of type Q (see Figure 6.2), a resistor first computed in [9]. The domain is enclosed by $B = [-3/2, 3/2] \times [-3/4, 3/4]$. There are two square holes (rotated by $\pi/4$)

$$H_1 = \{(-1/2, 0), (-3/4, 1/5), (-1, 0), (-3/4, -1/5)\},$$

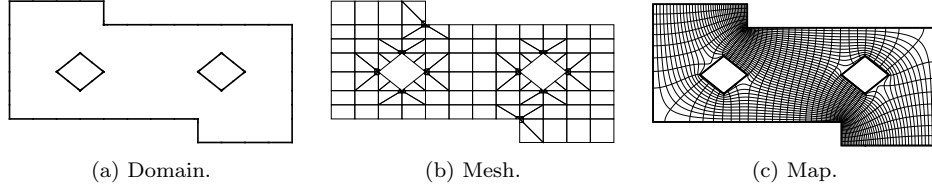


Fig. 6.2: Resistor.

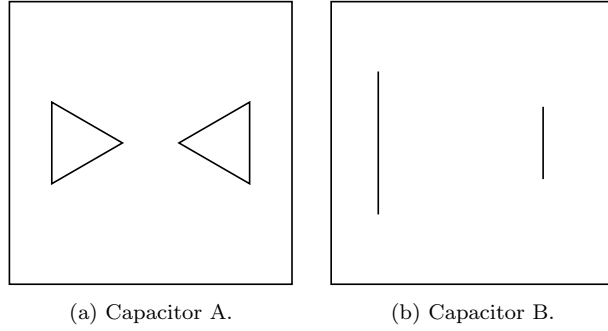


Fig. 6.3: Capacitors.

$$H_2 = \{(1/2, 0), (3/4, -1/5), (1, 0), (3/4, 1/5)\},$$

and indentations

$$I_1 = [-3/2, 1/2] \times [-3/4, -1/2], \quad I_2 = [-1/2, 3/2] \times [1/2, 3/4].$$

The domain $\Omega = B \setminus (H_1 \cup H_2 \cup I_1 \cup I_2)$. The contacts are on $x = -3/2$ and $y = -3/4$. The computed value of resistance $R = 2.841998463680$ is equal to that reported in [9].

6.1.3. Computation of capacities. We consider two cases, Capacitor A and B, examples 7 and 10 from [3], respectively (see Figure 6.3). In both cases the domain Ω is enclosed within $D = [-1, 1] \times [-1, 1]$. For Capacitor A, the plates are defined as the union of an equilateral triangle T and its reflection in the real axis. The vertices of T are the points $(a, 0)$, $(b, (b-a)/\sqrt{3})$ and $(b, -(b-a)/\sqrt{3})$, where $0 < a < b < 1$. Here $a = 1/5$ and $b = 7/10$ and the computed capacity $\text{cap}A = 9.49308124$ is within the estimated error of the reference value. For Capacitor B, the plates are two slits $\overline{A_s B_s}$ and $\overline{C_s D_s}$, defined by points $A_s = (-2/3, -1/2)$, $B_s = (-2/3, 1/2)$, $C_s = (1/2, -1/4)$, $D_s = (1/2, 1/4)$. The computed capacity $\text{cap}B = 8.47016014$ is also within the estimated error of the reference value.

6.2. Reference Cases. First we solve two standard problems up to very high accuracy in order to establish reference results for capacities in cases with symmetries. The domains are shown in Figures 6.4 and 6.5. In both cases the p -version converges exponentially as expected. The reference values for capacities are given in Table 6.2a.

| Experiment | Capacity | Error order | (Reference) |
|-------------------|----------------|-------------|-----------------|
| Interior contacts | 2.768867502692 | 12 | (2.76886750270) |
| Resistor | 2.841998463680 | 11 | (2.8419984) |

(a) Computed resistance.

| Experiment | Capacity | (Reference) | (Error) |
|-------------|------------|-------------|---------|
| Capacitor A | 9.49308124 | (9.4930811) | (4e-7) |
| Capacitor B | 8.47016014 | (8.4701600) | (5e-7) |

(b) Computed capacity. (Error) refers to the reported estimated error of the reference.

| Experiment | Mesh | DOF |
|-------------------|--------------------|--------|
| Interior contacts | (1569,2804,0,1280) | 187293 |
| Resistor | (667,1236,16,552) | 81935 |
| Capacitor A | (509,946,8,428) | 63143 |
| Capacitor B | (1013,1910,0,896) | 130439 |

(c) FEM-data: Mesh: (nodes, edges, triangles, quads); Degrees of freedom given at $p = 12$.

Table 6.1: Data on benchmarks.

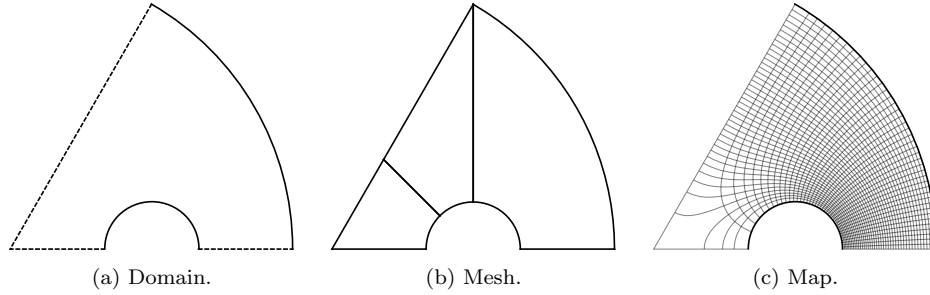


Fig. 6.4: Three Disks in Circle: Reference case 1.

6.3. Symmetric Case: Three Disks in Circle. Consider a unit circle with three disks of radius $r = 1/6$ placed symmetrically so that their origins lie on a circle of radius $r = 1/2$. As indicated in Figure 6.6a the cut can be computed analytically. The blending function approach used to compute higher order curved elements is very accurate if the element edges meet the curved edges at right angles. This is the reason for the mesh of Figure 6.6b where all edges adjacent to disks have been set optimally.

Notice that due to symmetry, the scaled jumps could also be computed analytically. In the numerical experiments only computed values of Table 6.2b are used, however. Since the cut is embedded in the mesh lines, both problems (the original and the conjugate) can be solved using the same mesh. In this optimal configuration convergence in reciprocal relation is exponential in p , which is a remarkable result, see Figure 6.7b. Similarly, in Figure 6.7a, it is clear that the derivatives have also converged over the whole domain.

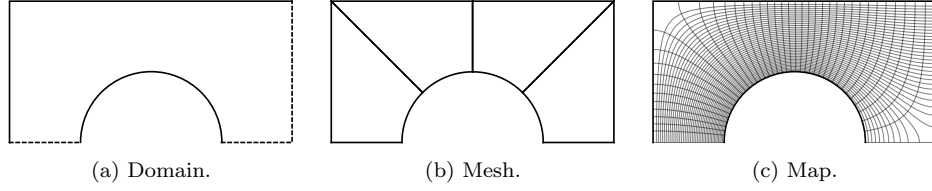


Fig. 6.5: Two Disks in Rectangle: Reference case 2.

| Case | Capacity | Error order |
|------|---------------|-------------|
| 1 | 1.61245904853 | 12 |
| 2 | 3.48074407477 | 12 |

(a) Reference capacities.

| Experiment | Capacity | Error order |
|----------------------------------|-----------------|-------------|
| Three Disks in Circle | 9.67475429123 | 12 |
| Two Disks in Rectangle | 13.922976299110 | 12 |
| Disk and Pacman in Rectangle | 13.3376294414 | 11 |
| Disk and Two Pacmen in Rectangle | 14.37(49228053) | 2 |

(b) Computed capacities.

| Experiment | Mesh | DOF |
|----------------------------------|--------------------|-------|
| Three Disks in Circle | (35, 52, 0, 18) | 2785 |
| Two Disks in Rectangle | (34, 49, 0, 16) | 2509 |
| Disk and Pacman in Rectangle | (181, 320, 4, 136) | 20377 |
| Disk and Two Pacmen in Rectangle | (353, 632, 8, 272) | 40657 |

(c) FEM-data: Mesh: (nodes, edges, triangles, quads); Degrees of freedom given at $p = 12$.

Table 6.2: R -type: Data on experiments.

6.4. Axisymmetric Cases. In the next two cases we maintain axial symmetry and thus analytic cuts. In both cases the enclosing rectangle $R = [-1, 3] \times [-1, 1]$.

6.4.1. Two Disks in Rectangle. Consider two disks of radius $= 1/4$ with centres at $(0, 0)$ and $(2, 0)$, respectively. The scaled jumps can be computed analytically, and standard jumps can be verified with the reference case 2 in Table 6.2a. Once again, the reciprocal convergence in p is exponential (see Figure 6.9c).

6.4.2. Disk and Pacman in Rectangle. Next the disk centred at $(2, 0)$ is replaced by a disk with one quarter cut, the so-called pacman. In this case we intentionally break the symmetry between meshes for the two problems. The geometric refinement at the re-entrant corners is done in slightly different ways. The reciprocal convergence in p is exponential, but with different rates at lower and higher values of p . Also, the difference in the number of refinement levels leads to mild consistency error which appears as loss of further convergence and accuracy at high p (see Figure 6.9d).

Here the jumps must be computed numerically (and tested against the computed

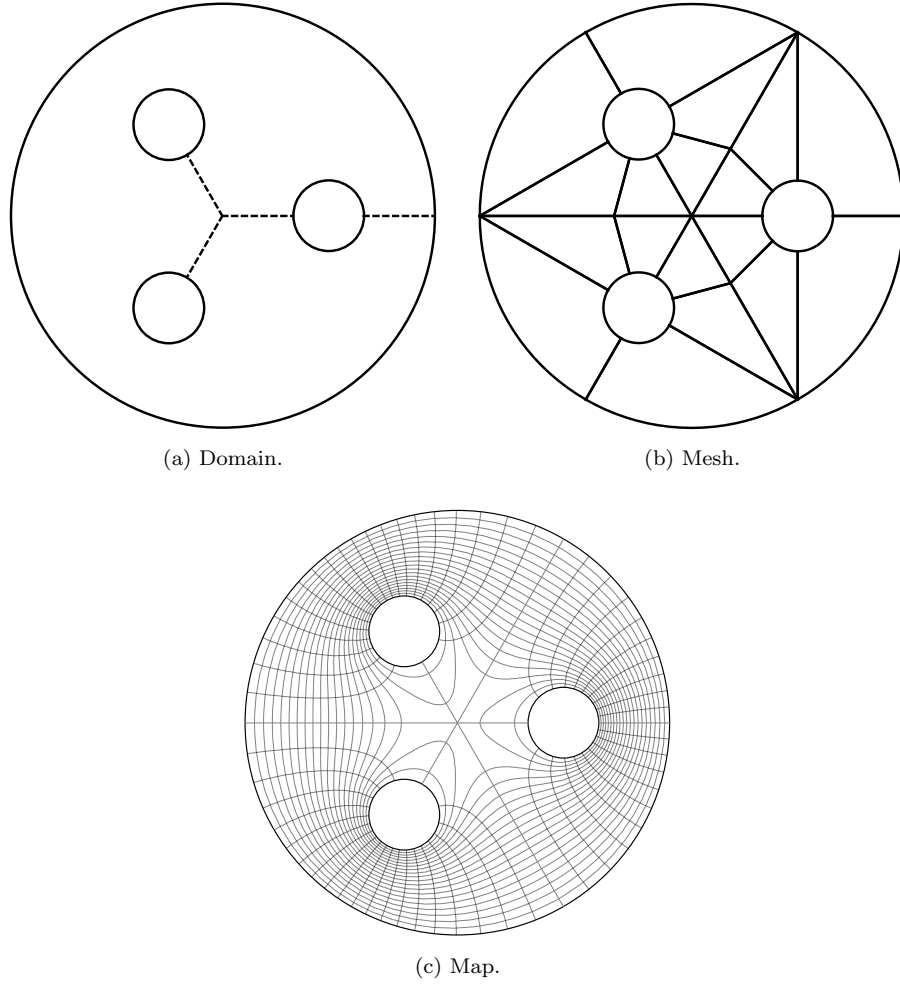


Fig. 6.6: *R*-type: Fully symmetric case.

capacity). Jumps are with four decimals:

$$d_1 = 3.4808, d_2 = 6.3761, d_3 = 3.4808.$$

7. Advanced Examples.

7.1. Disk and Two Pacmen in Rectangle. The first example in this section is a general one with enclosing rectangle $R = [-1, 3] \times [-1, 4]$ and one disk of radius $= 1/4$ at $(0, 1)$ and two pacmen at $(2, 0)$ and $(2, 3)$. In this case the cuts cannot be determined analytically. The effect of the cut in relation to the original problem can be seen by comparing the meshes of Figures 7.1a and 7.1b. One of the mesh points or nodes is moved to the saddle point and the corresponding edge has been aligned with the cut. As outlined before, the question of convergence in the reciprocal relation

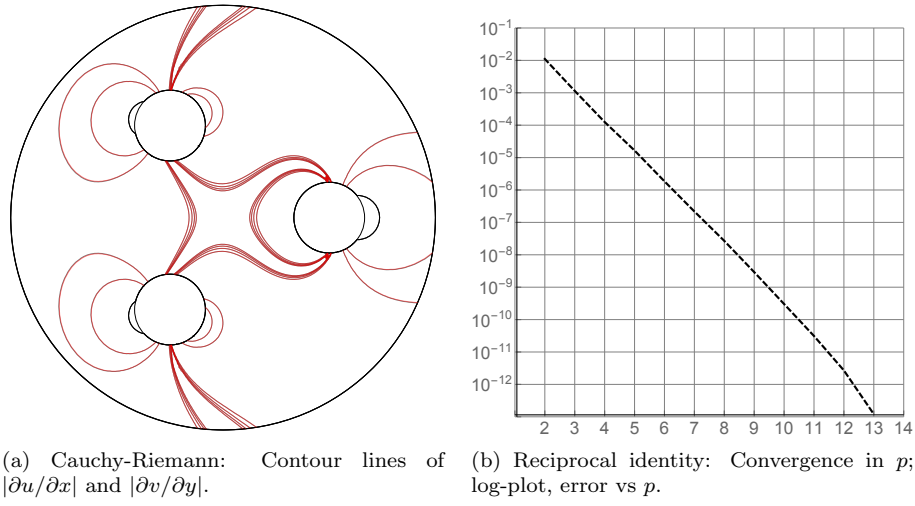


Fig. 6.7: R -type: Fully symmetric case.

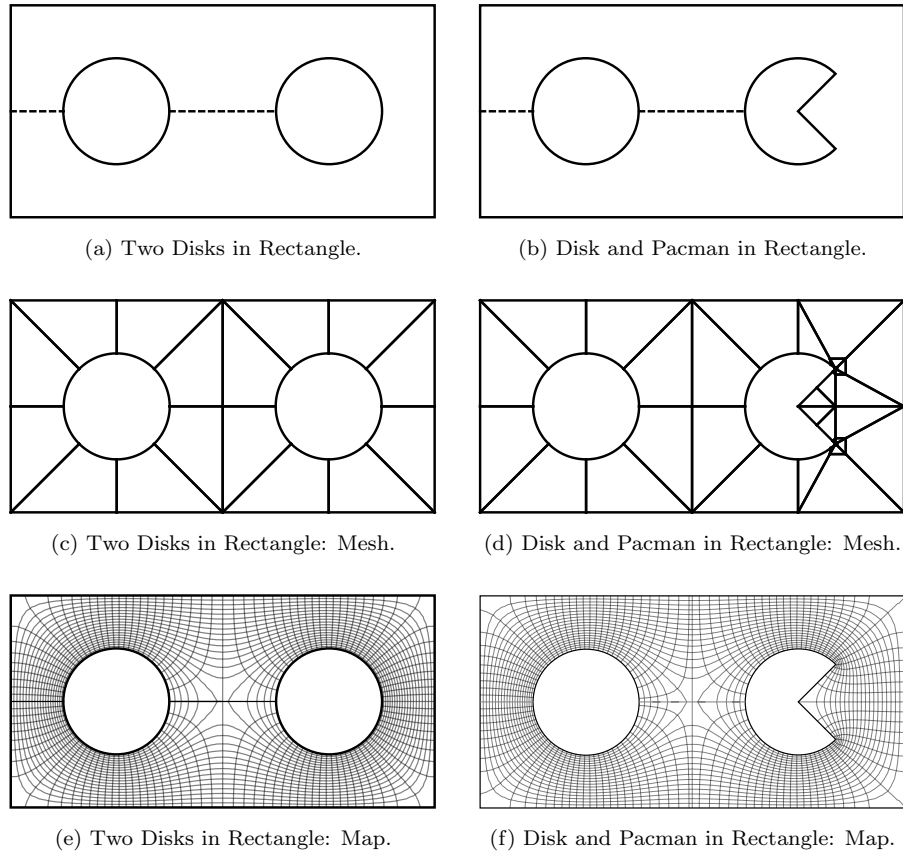


Fig. 6.8: R -type: Axially symmetric cases.

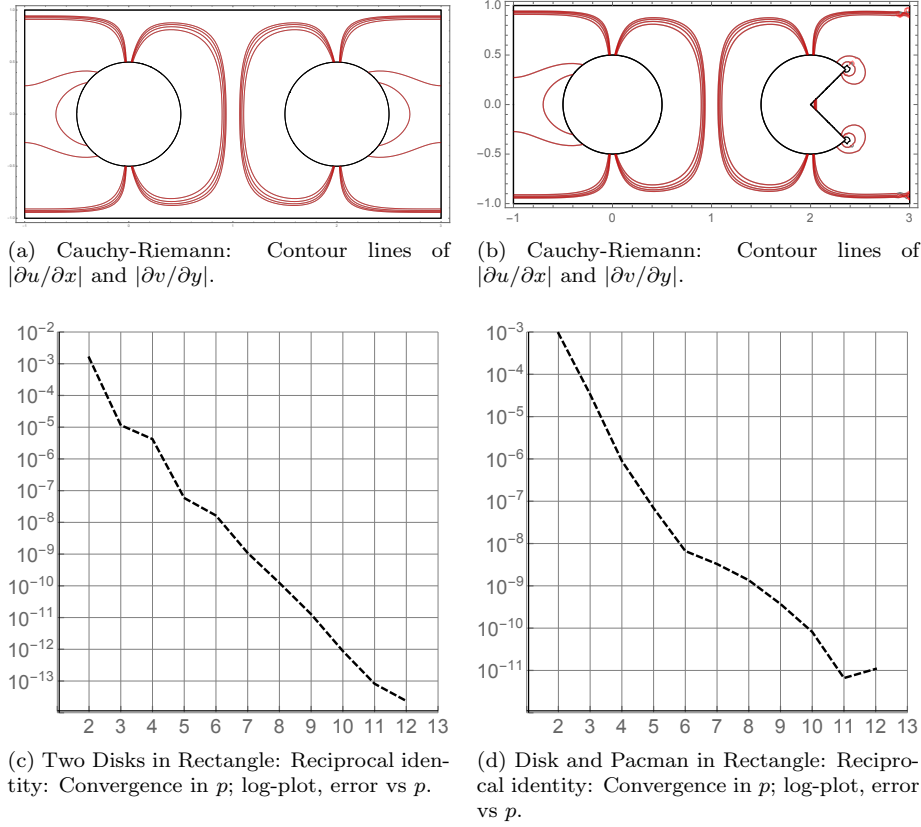


Fig. 6.9: R -type: Axially symmetric cases.

is somewhat ambiguous in this case. The smallest error in the given configuration is 0.00185. The jumps in the derivatives across the cuts are also clearly visible in Figure 7.1d. However, in Figure 7.1c we see how the contour lines do not cross the cuts except at the saddle points. Jumps are with four decimals:

$$d_1 = 2.0001, d_2 = 4.94015, d_3 = 0.09500, d_4 = 5.1651, d_5 = 2.1746.$$

REMARK 3. *In the Figure 7.1d the contour lines are given without any concern to the problem at hand. It would always be possible to, for instance, interpolate across the cuts and control the error. Here we have wanted to emphasize the effect of the approximate cut.*

7.2. Pacman and Droplet: Domain with Cusp. As next example we consider an axisymmetric case with a pacman from above and a domain bounded by a Bezier curve:

$$r(t) = \frac{1}{640} (45t^6 + 75t^4 - 525t^2 + 469) + \frac{15}{32} t (t^2 - 1)^2, \quad t \in [-1, 1].$$

In [14] a ring-domain with the same curve has been considered up to very high accuracy. Notice that the “droplet” is designed so that also the tangents are aligned for

parameter values $t = \pm 1$, thus the opening angle is 2π requiring strong grading of the mesh. The resulting maps are shown in Figure 7.2.

7.3. Perforated Domain: Domain with Uncertainty. One fascinating and new application for conformal maps is book-keeping of data in case of domains with uncertainty. Consider the perforated domain in Figure 7.3. Let us assume that in plane elasticity we are interested in stresses under fixed loading. If the manufacturing process leads to imperfections in the locations and sizes of the holes the task is to synthesize the stress fields over different realizations.

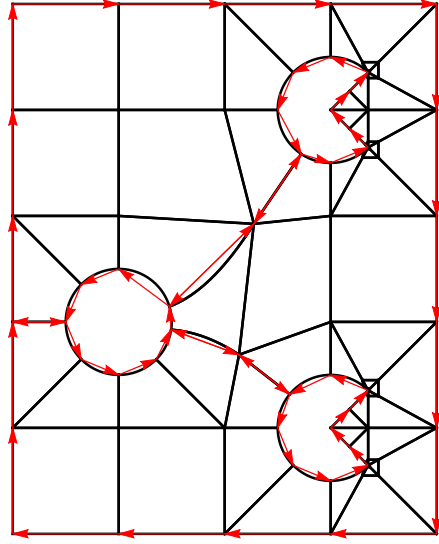
Let us refer to the domain without imperfections as the nominal domain (Figure 7.3a). The key observation is that once the canonical domain of the nominal domain has been computed, the canonical domains of all realizations can further be mapped onto that of the nominal domain. As a result of this for every point of the nominal domain a distribution of stresses is measured rather than a single value. This approach has been successfully applied in an industrial project where a simply connected domain with uncertain boundary was studied [22].

ACKNOWLEDGMENT 1. *The authors wish to thank prof. R. Michael Porter for his careful reading of an earlier version of this manuscript. The authors also wish to thank prof. T. DeLillo and Dr. E. Kropf for help in setting up the example of Section 6.1.2.*

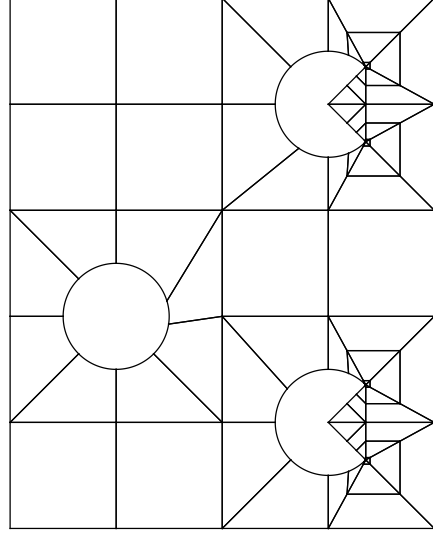
REFERENCES

- [1] L.V. AHLFORS, *Conformal invariants: topics in geometric function theory*, McGraw-Hill Book Co., 1973.
- [2] L.V. AHLFORS, *Complex Analysis*, An introduction to the theory of analytic functions of one complex variable, Third edition. International Series in Pure and Applied Mathematics. McGraw-Hill Book Co., New York, 1978.
- [3] D. BETSAKOS, K. SAMUELSSON, M. VUORINEN, *The computation of capacity of planar condensers*, Publ. Inst. Math. 75 (89) (2004), pp. 233–252.
- [4] D.G. CROWDY, *The Schwarz-Christoffel mapping to bounded multiply connected polygonal domains*, Proc. R. Soc. Lond. Ser. A Math. Phys. Eng. Sci. 461, no. 2061, 2653–2678, 2005.
- [5] D.G. CROWDY, *Schwarz-Christoffel mappings to unbounded multiply connected polygonal regions*, Math. Proc. Cambridge Philos. Soc. 142, no. 2, 319–339, 2007.
- [6] D.G. CROWDY, C.C. GREEN, *The Schottky-Klein prime function MATLAB files*, <http://www2.imperial.ac.uk/~dgcrowdy/SKPrime>, 2010.
- [7] D.G. CROWDY, J.S. MARSHALL, *Computing the Schottky-Klein prime function on the Schottky double of planar domains*, Comput. Methods Funct. Theory 7, no. 1, 293–308, 2007.
- [8] T.K. DELILLO, A.R. ELCRAT, J.A. PFALTZGRAFF, *Schwarz-Christoffel mapping of multiply connected domains*, J. Anal. Math. 94, 17–47, 2004.
- [9] T.K. DELILLO, A.R. ELCRAT, E.H. KROPP, *Calculation of Resistances for Multiply Connected Domains Using Schwarz-Christoffel Transformations*, Comput. Methods Funct. Theory 11, no. 2, 725–745, 2012.
- [10] T.A. DRISCOLL, *A MATLAB Toolbox for Schwarz-Christoffel Mapping*, ACM Transactions on Mathematical Software 22, no. 2, 168–186, 1996.
- [11] T.A. DRISCOLL, *Schwarz-Christoffel toolbox for MATLAB*, <http://www.math.udel.edu/~driscoll/SC/>
- [12] T.A. DRISCOLL, L.N. TREFETHEN, *Schwarz-Christoffel Mapping*, Cambridge Monographs on Applied and Computational Mathematics, 8. Cambridge University Press, 2002.
- [13] H. GRUNSKY, *Lectures on Theory of Functions in Multiply Connected Domains*, Vandenhoeck & Ruprecht, 1978.
- [14] H. HAKULA, T. QUACH, A. RASILA, *Conjugate Function Method for Numerical Conformal Mappings*, J. Comput. Appl. Math. 237, no. 1, 340–353, 2013.
- [15] H. HAKULA, A. RASILA, M. VUORINEN, *On moduli of rings and quadrilaterals: algorithms and experiments*, SIAM J. Sci. Comput. 33, no. 1, 279–302, 2011.

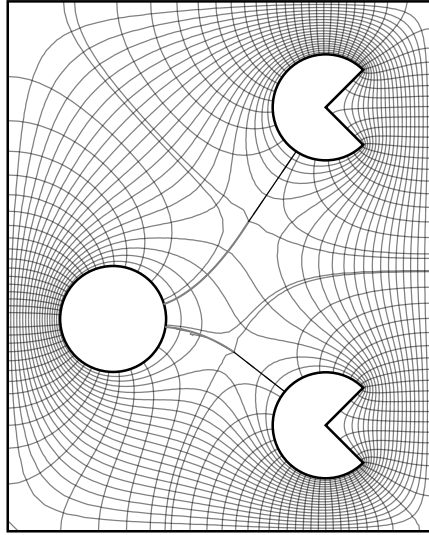
- [16] H. HAKULA, A. RASILA, M. VUORINEN, *Computation of exterior moduli of quadrilaterals*, Electron. Trans. Numer. Anal. 40, 436–451, 2013.
- [17] H. HAKULA, A. RASILA, M. VUORINEN, *Conformal modulus on domains with strong singularities and cusps*, Submitted to ETNA, 2016.
- [18] J.A. IADANZA, R. SINGH, S.T. VENTRONE, I.L. WEMPLE, *Method for designing an integrated circuit having multiple voltage domains*, US Patent 7,000,214, 2006.
- [19] I.V. IONOVA, E.A. CARTER, *Ridge method for finding saddle points on potential energy surfaces*, J. Chem. Phys. 98, no. 8, 6377–6386, 1993.
- [20] P. KOEBE *Abhandlungen zur Theorie der konformen Abbildung. IV. Abbildung mehrfach zusammenhängender schlichter Bereiche auf Schlitzbereiche*, Acta Math. 41, 1 (Dec. 1916), 305344.
- [21] O. LEHTO, K.I. VIRTANEN, *Quasiconformal mappings in the plane*, Springer, Berlin, 1973.
- [22] J. LEHTONEN *Collocation method for solving stochastic elasticity problems with an uncertain domain*, M.Sc Thesis, 2015.
<https://aaltodoc.aalto.fi/handle/123456789/15338>
- [23] W. LUO, J. DAI, X. GU, S.-T. YAU, *Numerical conformal mapping of multiply connected domains to regions with circular boundaries*, J. Comput. Appl. Math. 233, no. 11, 2940–2947, 2010.
- [24] A. MAYO, *Rapid methods for the conformal mapping of multiply connected regions*, J. Comput. Appl. Math. 14, no. 1-2, 143–153, 1986.
- [25] Z. NEHARI, *Conformal Mapping*, McGraw-Hill Book, New York, 1952.
- [26] N. PAPAMICHAEL, N.S. STYLIANOPOULOS, *Numerical Conformal Mapping: Domain Decomposition and the Mapping of Quadrilaterals*, World Scientific Publishing Company, 2010.
- [27] L. REICHEL, *A fast method for solving certain integral equations of the first kind with application to conformal mapping*, J. Comput. Appl. Math. 14, no. 1–2, 125–142, 1986.
- [28] O. SÉTE, J. LIESEN, *On conformal maps from multiply connected domains onto lemniscatic domains*, ETNA, Volume 45, pp. 1–15, 2016.
- [29] L.N. TREFETHEN, *Numerical computation of the Schwarz-Christoffel transformation*, SIAM J. Sci. Statist. Comput. 1, no. 1, 82–102, 1980.
- [30] L. N. TREFETHEN, *Analysis and design of polygonal resistors by conformal mapping*, ZAMP 35, 692–704, 1984.



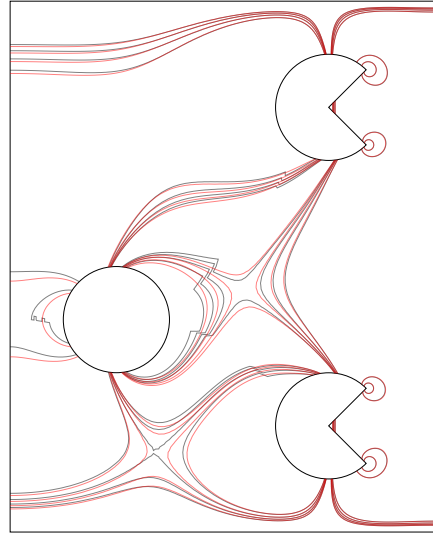
(a) Domain.



(b) Mesh.

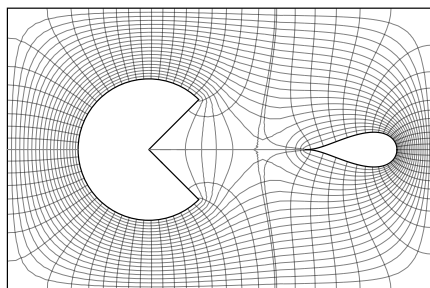


(c) Map.

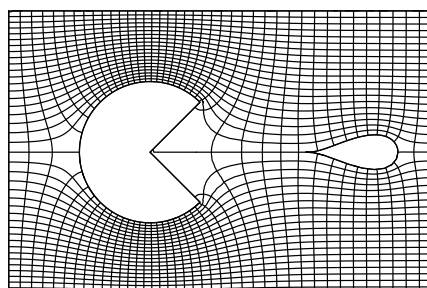


(d) Cauchy-Riemann: Contour lines of $|\partial u/\partial x|$ and $|\partial v/\partial y|$.

Fig. 7.1: *R*-type: Disk and Two Pacmen in Rectangle. Contour lines, in d, of derivatives are given without any concern to the problem at hand. Thus jumps across the cut are clearly visible. It is possible to interpolate across the cuts and control the error. Here we have left the jump to emphasize the effect of the approximate cut.

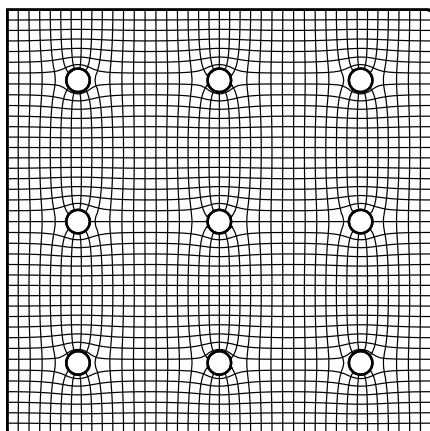


(a) R -type: Map.

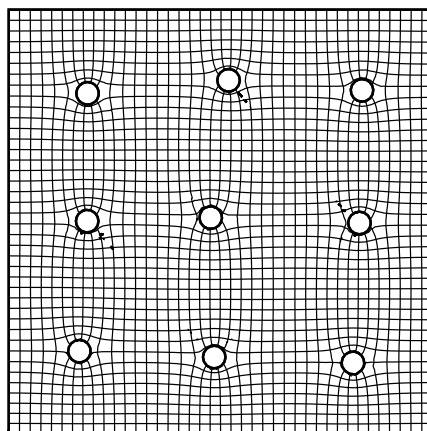


(b) Q -type: Map.

Fig. 7.2: Pacman and Droplet.



(a) Nominal domain: Map.



(b) Perturbed domain: Map.

Fig. 7.3: Q -type: Perforated System.